Grant agreement no. 312818

SPA.2012.2.2-01 : Key technologies enabling observations in and from space

- Collaborative project -

D2.1
Candidate key technologies trade-off study

WP 2 - Interferometer satellite Technology Development

Due date of deliverable: month 13

Actual submission date: February 3rd 2014

Start date of project: January 1st 2013   Duration: 36 months

Lead beneficiary for this deliverable: CNRS - LAM

Last editor: S. Vives, Laboratoire d'Astrophysique de Marseille (CNRS-LAM)

Contributors:
K. Dohlen (CNRS-LAM), V. Iafolla (AGI), E. Rakotonimbahy (CNRS-LAM), G. Savini (UCL)

Project co-funded by the European Commission within the Seventh Framework		
Dissemination Level (please refer to the list of deliverables in Annex 1 and complete		
PU	Public	■
PP	Restricted to other programme participants (including the Commission	
RE	Restricted to a group specified by the consortium (including the	
CO	Confidential, only for members of the consortium (including the Commission Services)	

History table

Version	Date	Released by	Comments
1	31/01/2014	LAM-CNRS	First issue

Table of contents

Acknowledgements

Disclaimer

The content of this deliverable does not reflect the official opinion of the European Union. Responsibility for the information and views expressed in the deliverable therein lies entirely with the author(s).

1   Introduction

1.1   General context

Space-born testing of key technologies, as offered by a nano-satellite mission, will be an important ingredient to improve the FIRI Technology Readiness Level (TRL).

Task 2.3 is dedicated to the validation of one key technology of FIRI with nano-satellite. In this task, the possibilities for technological validation offered by a nano-satellite-born test bench will be considered and a selection of FIRI key technologies benefiting from such validation will be identified. The technology validation test-bench and its associated support equipment will be specified and subsequently developed (optics, mechanics, and electronics). In parallel, the nano-satellite concept will be studied and implemented.

1.2   Deliverable objectives

The main objectives of this deliverable are 1) to assess the possibilities for technological validation offered by a nano-satellite-born test bench; and 2) to identify and select the FIRI key technology benefiting from such validation.

The first part of this report defines the concept of nano-satellite and describes the resources (mass, volume, power, telemetry) typically available on a nano-satellite for the payload. The second part is dedicated to the selection of the FIRI key technology which will be studied and implemented on a nano-satellite in the next phases.

2   Description of activities and research findings

2.1   Nanosatellite and Cubesat Overview

The nanosatellite shall provide a validation test in space for a key technology of FIRI. In this section, the main characteristics of the nanosatellite and resources available for the payload are described.

One reason for miniaturizing satellites is to reduce the cost: while classical satellites require large and costy rockets, smaller and lighter satellites require smaller and cheaper launch vehicles and can sometimes be launched in multiples. They can also be launched in 'piggyback', using excess capacity of launch vehicles.

Besides the cost issue, the main rationale for the use of miniaturized satellites is the opportunity to enable missions that a larger satellite could not accomplish, such as:

- Constellations for low data rate communications
- Using formations to gather data from multiple points
- In-orbit inspection of larger satellites.
- University Related Research

2.1.1 Nanosatellite

The term "nanosatellite" or "nanosat" is applied to an artificial satellite with mass between 1 and 10 kg. For example, Figure 1 (left) shows the nanosat called WebSat which was developed by Ecole Polytechnique Fédérale de Lausanne. It is a 3 kg nanosatellite which is intended to broadcast Earth pictures on-line in real time from a 400 km Sun synchronous orbit.
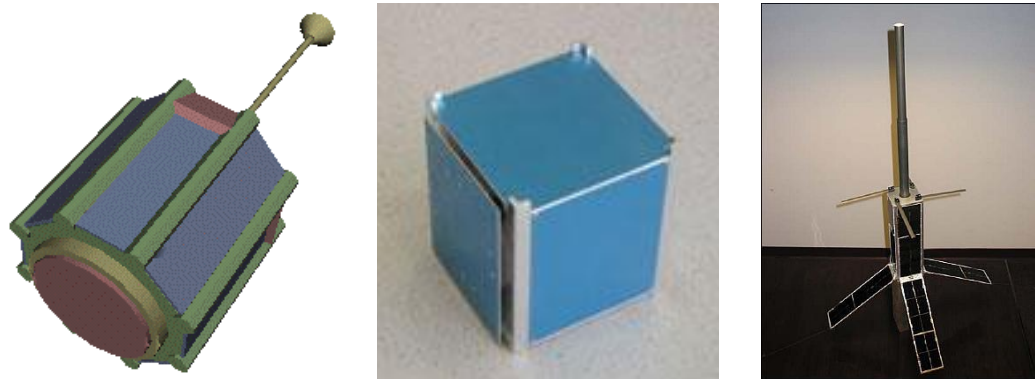

Figure 1 – LEFT: 3D view of WebSat: a nanosatellite broadcasting Earth pictures on-line in real time. MIDDLE: Picture of Cute-I, a 1U cubesat developed to tests commercial components. RIGHT: Picture of Quake Sat, a 3U cubesat developed to detect low frequency emissions during Earthquakes.

2.1.2 Cubesat

2.1.2.1 Cubesat Definition

A cubesat is a type of nanosatellite for space research that usually has a volume of exactly one liter (10 cm cube), has a mass of no more than 1.33 kilograms, and typically uses commercial off the-shelf (COTS) components for its electronics.

Beginning in 1999, California Polytechnic State University (Cal Poly) and Stanford University developed the cubesat specifications to help universities worldwide perform space science and exploration. The cubesat specification accomplishes several high-level goals. Simplification of the satellite's infrastructure makes it possible to design and produce a workable satellite at low cost. Encapsulation of the launcher-payload interface takes away the prohibitive amount of managerial work that would previously be required for mating a piggyback satellite with its launcher. Unification among payloads and launchers enables quick exchanges of payloads and utilization of launch opportunities on short notice.

The term "CubeSat" was coined to denote nanosatellites that adhere to the standards described in the cubesat design specification. Cal Poly published the standard in an effort led by aerospace engineering professor Jordi Puig-Suari. The specification does not apply to other cube-like nanosatellites such as the NASA "MEPSI" nanosatellite, which is slightly larger than a cubesat.

In 2004, with their relatively small size, cubesats could each be made and launched for an estimated $65,000–$80,000. This price tag, far lower than most satellite launches, has made cubesat a viable option for schools and universitie. Because of this, a large

number of universities and some companies and government organizations around the world are developing cubesats — between 40 and 50 universities in 2004, Cal Poly reported.

As example, Figure 1 (Middle and right) shows two cubesats: Cute – I (developed by Tokyo Institute of Technology) and Quake Sat (developed by Stanford University), a 1U cubesat and a 3U cubesat respectively. The first one is designed to test COTS components whereas the second one aims to detect extremely low frequency radio emission of seismic activity during earthquakes.

2.1.2.2 Cubesat Unit

The standard 10×10×10 cm basic cubesat is often called a "1U" cubesat meaning one unit. Cubesats are scalable along only one axis, by 1U increments, allowing for simple implementation of "2U" (20×10×10 cm) and "3U" (30×10×10 cm) cubesast.

2.1.2.3 Cubesat deployment system

Since cubesats all have cross-section 10x10 cm regardless of length, they can all be launched and deployed using a common deployment system. Cubesats are typically launched and deployed from a mechanism called a Poly-PicoSatellite Orbital Deployer (P-POD), also developed and built by Cal Poly. The P-POD is a rectangular box with a door and a spring mechanism, as shown Figure 2.

P-PODs are mounted to a launch vehicle and carry cubesats into orbit and deploy them once the proper signal is received from the launch vehicle. P-PODs have deployed over 90% of all cubesats launched to date (including un-successful launches), and 100% of all cubesats launched since 2006. The P-POD Mk III has capacity for three 1U cubesats. Since three 1U cubesats are exactly the same size as one 3U cubesat, and two 1U cubesats are the same size as one 2U cubesat, the P-POD can deploy 1U, 2U, or 3U cubesats in any combination up to a maximum volume of 3U.
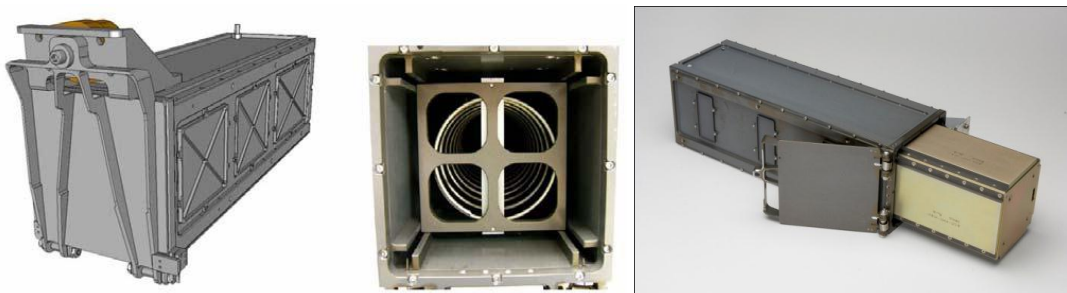
Figure 2 – Cubesat deployment system P-POD

2.1.2.4 Cubesat background

The first cubesats were launched in June 2003 on a Russian Eurockot, and approximately 75 cubesats have been placed into orbit since August 2012. We have elaborated a statistical survey of success rate based on available data. Unfortunately, for many cubesat missions insufficient detail is available to be considered in our survey. Figure 3 shows the status of 66 well-documented cubesat missions.

Overall, 66% of these missions have succeeded. In 2006, 14 cubesats were destroyed due to launch failure (the launch vehicle disintegrated during launch). For the rest, the failure is resulting from a communication problem.
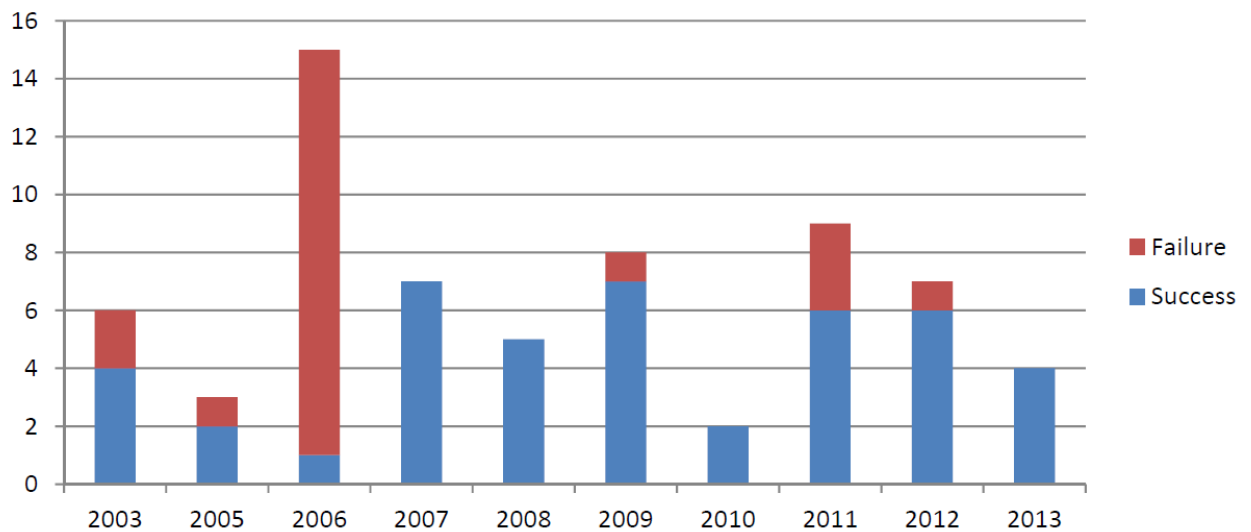

Figure 3 – Cubesat missions success statistics.

2.1.2.5 Cubesat main characteristics

The purpose of the cubesat project is to provide a standard for design of nanosatellites to reduce cost and development time, increase accessibility to space and sustain frequent launches.

Table 1 sums up the main characteristics of the past 10 years missions and gives us a glimpse of what can be done with cubesats.

Table 1 – Summary of main characteristics of cubesat missions since 2003.

Total mass	0,8 kg to 7,5 kg
Available power	0,3 W to 11,5 W
Total volume	1 dm^3 to 8 dm^3
Payload mass	30 % to 62,7 %
Payload power consumption	Up to 83 %
Payload volume	50 % to 60 %
Telemetry	15 bps to 256 kbps
Expected lifetime	From 21 days to 3 years
Nominal lifetime	Up to 6 years
Orbit	LEO from 350 km to 1.450 km
Development time	From 7 months to 5 years
Person assigned to the program	6 to 200

More details about cubesats and missions are available at:
- http://mtech.dk/thomsen/space/cubesat.php#3
- http://www.utias-sfl.net/nanosatellites/CanXProgram.html
- https://directory.eoportal.org/web/eoportal/satellite-missions

2.2   Cubesat Specifications

Following a thorough study of available COTS components and their cost and performance, we have elaborated cubesat platforms of type 1U, 2U and 3U, see Figure 4. This section defines the main interfaces and available resources for the payload hosted by each one of these options. The proposals for technology validation experiments should meet these specifications.
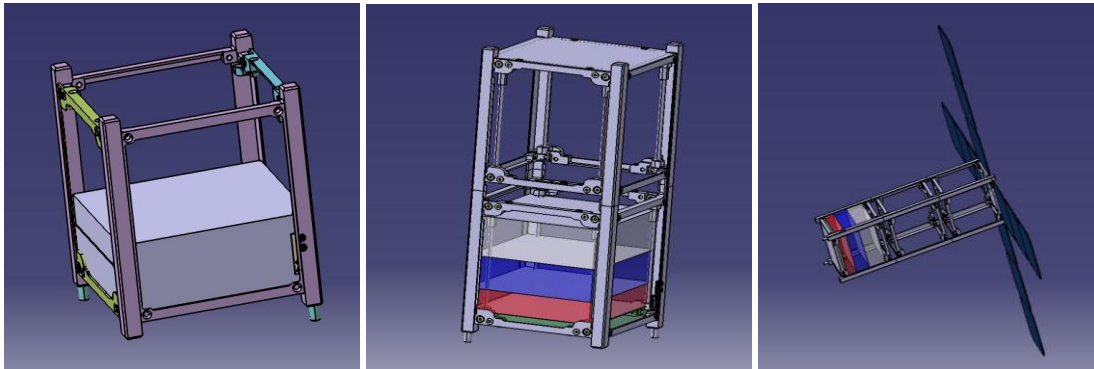

Figure 4 –Cubesat platforms of type 1U, 2U and 3U proposed for the FISICA study.

2.2.1   General Requirements

- All parts shall remain attached to the cubesat during launch, ejection and operation. No additional space debris shall be created.
- Pyrotechnics shall not be permitted.
- No pressure vessels over 1.2 standard atmosphere shall be permitted.
- Pressure vessels shall have a factor of safety no less than 4.
- Total chemical energy shall not exceed 100 watt-hours.
- Total Mass Loss (TML) shall be ≤ 1.0%
- Collected Volatile Condensable Material (CVCM) shall be ≤ 0.1%

2.2.2   Cubesat Physical Requirements

- Cubesat physical characteristics shall meet the specifications listed in Table 2.
- The cubesat center of gravity shall be located within a sphere of 2 cm from its geometric center.

Table 2 – Cubesat height and mass

	1U	2U	3U
Base	100 x 100 mm	100 x 100 mm	100 x 100 mm
Height	113.5±0.1 mm	227.0±0.2 mm	340.5±0.3 mm
Maximum weight	1.33 kg	2.66 kg	4.00 kg

2.2.3   Interface with payload and performance

- The payload shall operate using unregulated power, 3.3V or 5.5V

- The payload characteristics shall be compliant with the specifications listed in table 5.3. These specifications derived from configurations based on off-the-shelf equipment compatible with our top level needs.

Table 5.4 gives the attitude capabilities corresponding to the chosen cubesat configurations.

Table 3 – Payload Characteristics

	1U	2U	3U
Payload dimensions	98.4 x 98.4 x 44 mm	98.4 x 98.4 x 110 mm	98.4 x 98.4 x 210 mm
Payload maximum weight	390 g	1310 g	2650 g
Nominal payload power consumption	0.46 W	1.66 W	3.36 W
Peak payload power consumption	0.6 W	1.8 W	3.5 W

Table 4 – Cubesat Attitude Capabilities

	1U	2U	3U
Best Attitude knowledge accuracy	5 deg	9.10^{-3} deg	9.10^{-4} deg
Best Attitude control accuracy	10 deg	6.10^{-2} deg	3.10^{-4} deg

2.3 Overview of the potential key technology fields

2.3.1 Formation Flying

Formation Flying (FF) is the concept of flying multiple satellites in a desired geometry to synthesize the function of a large virtual instrument. The initial FIRI proposal suggested using 3 telescopes separated by several hundreds of meters, even up to 1 km.

The scope for using Formation Flying is broad, but all formation flying missions have the following main generic features: the number of satellite is larger than one, the satellites operate in relative proximity, and relative motion control constraints must be applied to maintain the formation.

In the case of FIRI, the satellite relative motion will be determined principally by spacecraft propulsion. This type of formation is called "Non-Keplerian". The satellites are controlled autonomously on-board: the relative position and attitude are controlled in closed-loop based on relative metrology systems between the spacecraft.

A representative demonstration of FF (involving relative metrology, micro-propulsion, guidance and navigation control in closed-loop including safe deployment, reconfiguration, collision avoidance …) is not feasible with our time and resources.

It is worth noting that the purely technological mission PRISMA launched in 2010 has already demonstrated the capability of two satellites to operate in formation.

However, cubesats could be used to validate elementary bricks involved in the formation flying.

Regarding the relative metrology, it exists typically 3 complementary classes of accuracy:

- Centimeter Class (coarse metrology): this accuracy is achieved with Radio Frequency (RF) metrology systems. Such systems have been validated (TRL9) on-board PRISMA.
- Millimeter Class (fine metrology): this metrology is achieved by using optical systems. These optical systems differ in function of the FF configuration.
- Micrometer Class (accurate metrology): this metrology is mainly achieved by laser interferometry.

All these systems are already under development and/or validation in laboratories and industries. Usually their physical characteristics are not compatible with the available resource of a cubesat.

In conclusion, except for novel elementary bricks (such as the accelerometer, see Proposal A) the use of cubesat for FF demonstration seems too challenging and not realistic in the FISICA timeframe.

2.3.2 Pointing and positioning

Pointing accuracy is vital for FIRI. Technology in this field is fairly advanced and it might be perceived that there is not much that a cube-sat can do to improve this with the limited Attitude Control and Positioning. An alternative form of motion could perform vital testing in prolonged microgravity conditions. Proposal B (Section 2.4.2) corresponds to this category.

2.3.3 Telescope dishes

FIRI will require large telescopes. There is existing heritage for specific materials in Primary and Secondary mirrors of existing and planned space telescopes. With nanosatellites, potential new mirror materials or miniaturized deployable mechanisms could be tested. However, the testing referred to here should be that which cannot be performed in a space-like environment on the ground.

2.3.4 Mechanisms (delay lines)

Cubesat does not offer much in terms of distance. But micro-gravity could allow a noise-test on certain mechanisms in representative conditions. The Proposal A corresponds to such a validation.

2.3.5 Relevant optical techniques

Space-based astronomical observations are until now done using single-dish devices. The upcoming James Webb Space Telescope (JWST) is also a single-dish telescope although the use of segmentation introduces new problems of alignment and phasing of individual mirrors. The use of multiple-dish systems will be required in order to achieve the next step in angular resolution, beyond what can be achieved with JWST-style single-dish devices. Significant studies of multi-dish systems have already been done (SIM, Darwin, TPF, FIRI, …), but so far none of these concepts have been selected for construction and launch. While technological readiness of key elements like

deployment, formation keeping, etc clearly constitute major risks, more conceptual issues are also seen as risk elements. Will a multi-dish system provide useful scientific images? A demonstration of a multi-dish concept, even on a miniature platform, would therefore in itself be of interest.

2.4   Potential candidates

In order to identify the appropriate payload for the nanosatellite testbed, an internal "call for Payload proposals" has been opened in the consortium. The FISICA team proposed four technical solutions that are reproduced in the next sections.

2.4.1   Proposal A: An accelerometer as key element of a FIRI control loop

2.4.1.1 Scope

This proposal describes the main concept of a nanosatellite testbed to demonstrate the use of an accelerometer as fundamental element of the Formation Flying control loop.

2.4.1.2 Context

The FIRI interferometer will be placed in the Lagrange point L2 and maintained in this position by means of traditional techniques of attitude control, at which will also be entrusted the task to point the telescope to the sources. In the next phase of operation of the interferometer, it will rotate around the axis passing through the sources and for its HUB (axis ILSHUB), reducing the distance between the two outer satellites telescopes (R1(t), R2(t)), see Figure 5, so to cover the uv plane.

In a first idea the two satellites go through a spiral at a constant tangential velocity (about one meter in 25sec) with an appropriate control law that will govern the distance between the two telescopes and the rotation speed of the interferometer, so to ensure maximum coverage of the uv plane, in respect of its functionality from both the spatial and spectroscopic point of view; it is clear that also other modalities to cover the u,v plane will be considered, as for example to readjusting the satellites baseline every half turn. In L2 the dominant accelerations acting on the interferometer are essentially the inertial accelerations, determined by its rotation, in particular the centrifugal accelerations are of the order of 10^{-3}g. The measurement of these accelerations with precision 10^{-8}g, should allow the control of the system (this at least for the tethered and booms connection between the two telescopes) through the variation of the distance between the two satellites, its rotation and according to the law of conservation its momentum. The variations of these accelerations are expected at periods of about 24 hours, which represent the estimated time to walk the spiral so to cover the entire plane u, v. Also, we can underline the fact that the difference between the two measured accelerations is connected to the angular system rotation and to the distance between the two points at which the radial accelerations are measured:

$$a_d = \omega(t)^2 \cdot R(t) \text{ where } R(t) = R_1(t) + R_2(t)$$

Formula that gives the opportunity to recover the absolute distance between the two telescopes, if ω is measured (star sensors or gyroscope).
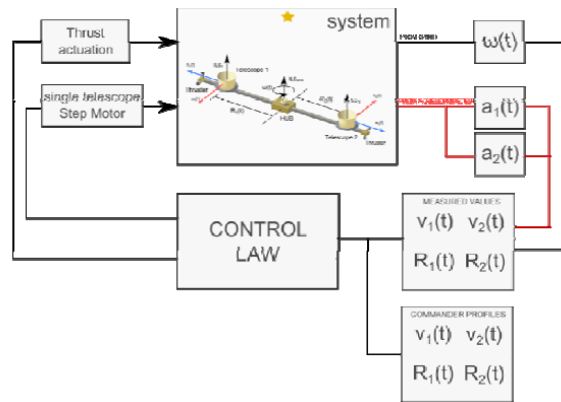

Figure 5 – Possible scheme of the interferometer control loop.

2.4.1.3 Technology

What we want to propose is the test of a single sensitive axis accelerometer, which has characteristics close to those that must be obtained in the interferometric mission. In terms of signal levels, it is thought that the orbiting nanosatellite has sufficiently low noise levels, so as to verify the precision of the accelerometer, while we trust in quite "big" acceleration present in the phases of its insertion in orbit so to verify the functionality at a high level. A more complex test is to verify the frequency response of the accelerometer; due to the low power to disposition in the nanosatellite, it is not possible to use a temperature control system, so the accelerometer will have a spurious response in temperature that could mask the low frequencies accelerometric signal, to mitigate these effects the accelerometer will be accompanied with a thermometer which should allow in part the reductions of these effects. The preliminary analysis of the characteristics of the nanosatellite seems to indicate its suitability for this test, both for the mechanical and electrical interfacing point of view.

In Table 5 are reported the characteristics of the single axis accelerometer, while in Figure 6 are reported its mechanical and its electrical parts.

Table 5 – Single axis accelerometer characteristics.

|	
Sensitivity	da 1e-7 a 1e-8 g/sqrt(Hz)
Acquisition frequencies (Hz)	0.1,0.2,0.5,1,5,10,20,50,100
Output	Analogic or digital
Data rate (10Hz one acc. And one T) [byte/s]	250
Internal thermometer Pt10000	Precision better than 10^{-4} °C
Interface of communication	Rete RS232 full-duplex/Rete RS485 (con adattatore)
Standard of communication	NMEA
Dimensions of a single axis mechanical element	80 x 60 x 25 (H x L x A)
Electronic dimensions for a single element [mm]	75X55X12
Voltage supply via USB or external [V]	5
Power dissipation	75 mW
Weighs [Kg]	0.200
Linearity	> 80 dB
Internal memory	SD 2Gb
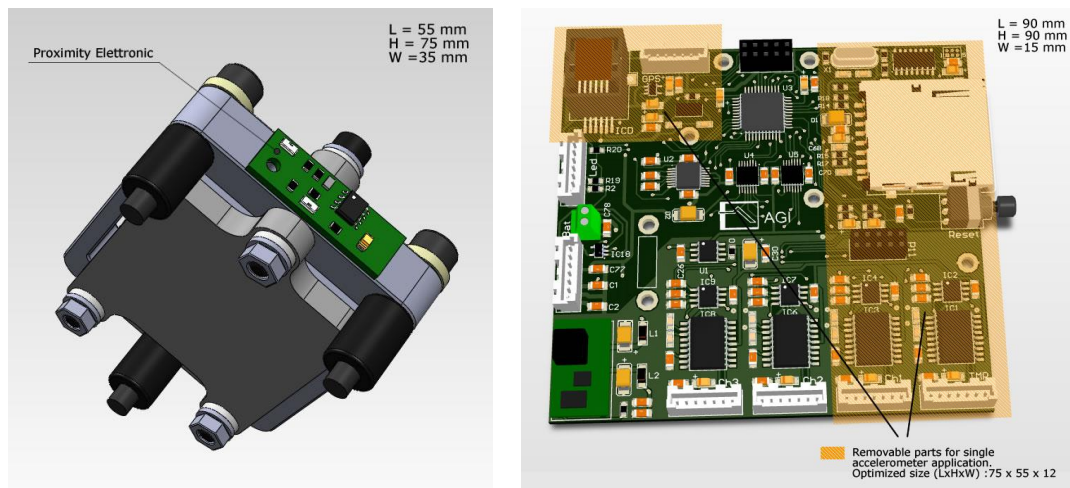
Figure 6 – LEFT: Mechanical part of the accelerometer. RIGHT: Electronic part of the accelerometer.

2.4.2   Proposal B: Thermal emission/absorption steering

2.4.2.1 Rationale

ETE-Enhanced Thermal Emission could be considered as a viable means for micro-steering when produced at the extremities of a long connected structure and in opposite directions. The scope is to attempt to micro-steer by controlling the temperature and/or the emission of purposely defined satellite surfaces.

2.4.2.2 Relevance

Long baseline structures requiring micro-pointing corrections could benefit by applying small amounts of torque to the structure via differential radiative emission (or differential response to photon pressure). This could produce non-negligible savings in the consumption of hydrazine (commonly used for spacecraft steering). The latter is the most efficient propellant and is also a very dangerous and toxic substance which

has been on a list for both ESA and NASA for research of a suitable alternative due risks in its preparation.

2.4.2.3 Method/Technique

Different locations in space are subject to different amounts of solar wind and Sun-related photon pressure. While in Pioneer-like surroundings thermal emission might be the dominant source of non-gravitational acceleration, in L2 and more so in LEO this will not be the case. To study the effects of variations in thermal emission with the purpose of specific accelerations the cube-sat should be designed in a way to either strike a balance between the solar photon pressure, the Earth's thermal emission and the cube-sat self-emission, or to make sure such contributions can be differentiated. The cube-sat is placed in a decaying orbit so there will be virtually no control on satellite trajectory and the acceleration will be constantly varying, but a 2U or a 3U (which offers a higher degree of attitude accuracy) could perform tests where we attempt to impart angular momentum along an axis orthogonal to the cubesat elongation (lower energy required). If electro-chromia (property of changing color by application of an electric field) is achieved (even minimally), differential acceleration could be measured with respect to solar photon pressure (on the dayside) and due to combined thermal emission/absorption of Earth thermal emission (on the night side).

There are two main ways in which this could be attempted: controlling either the surface temperature or the surface emission (or both). Ultimately both techniques will require power. Post-launch the satellite will begin thermalization and this will be modelled accurately in order to account for this as well as for the decaying orbit acceleration. Surface temperature can be easily controlled by active Joule dissipation while surface emissivity is more challenging. A "simple" active mechanism that allows a single (IR black/white) panel rotation would produce maximal effect. The scenario where small versions of such a mechanism are placed on a more complex satellite is not as attractive due to the added complexity of many small moving parts. An alternative is an IR version of electro-chromia which could have interesting applications per se.

2.4.2.4 Orders of magnitude of effects:

1-Solar photon pressure: Given the solar constant and an area of exposure of the two panels of interest (at the sides of a 3U) of A=0.01 cm2 each, the momentum imparted to such panel from the solar photon pressure is 5e-8 Ns on absorption and twice that on total reflection. Hence if we assume that we have a starting emissivity of 0.5 on two panels and that we can electronically alter these by only 0.1 in opposite ways (0.4 vs 0.6), we will obtain a torque of ~10-9 Nm (for 1kg units). Application of this torque for 10 minutes should produce a rotation of the unit of ~5 arcminutes which is easily monitored within the pointing accuracy and control.

2-Thermal emission from Earth: Calculations using an Earth blackbody radiative temperature of ~230K shows a photon pressure generally a factor 10 smaller with respect to contribution #1. While this is measureable, a general homogeneity in the cubesat panels facing Earth should allow us to neglect this effect.

3-Controlled Emission via Joule dissipation: Assume that a panel is mounted (Figure 7, right) with a weak thermal link to the cube-sat and that we can dissipate 1W of Joule power relatively uniformly (this can be achieved using a thin graphite sheet glued on a

layer of printed electronic dissipators. Given the numbers in appendix for the structure and weight of the panel, a differential temperature of ~20K should be achieved between a satellite T of 250K and the panel which could provide a torque between a factor 5 and 10 smaller than that of case #1. This could hence be easily tested by having homogeneous emissivity on all panels (thereby cancelling most of #1 and #2) and applying such power.

4-Atmospheric drag: This is by far the strongest force acting on the satellite with the worst case imparting an estimated 10uN at a 300km orbit. This is 3 to 4 orders of magnitude greater than the momentum created by photon pressure or emission. While a specific calculation will depend on the actual entire structure geometry, this will be an almost constant force which should not vary on short time constants and could be hence separated when monitoring the units' position and orientation.
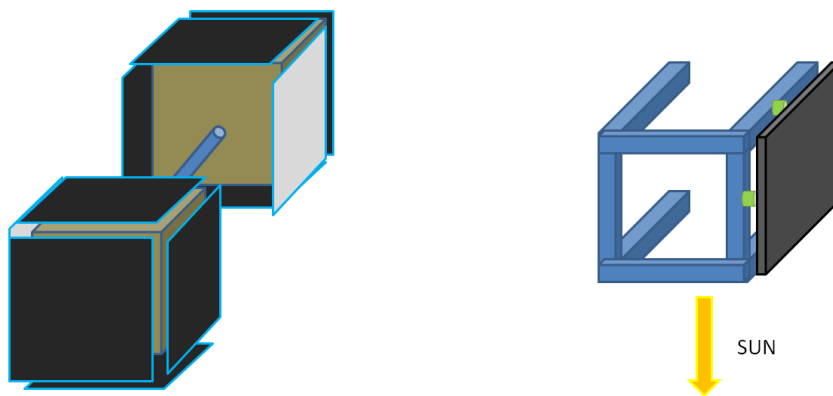

Figure 7 – LEFT: A 3U concept (for maximum AC and sensitivity to torque) where the surface emissivity (either controlled or pre-established) is purposely asymmetric to generate torque on the structure via either photon absorption/reflection or thermal emission. RIGHT: A single panel is heated to produce differential thermal emission and impart torque (note: all faces of cube would identical panels to balance photon pressure from both Sun and Earth).

2.4.2.5 Technology

Temperature control is substantially easier as it involves the use of printed electronic circuits which can be glued/mounted at the back of high-emission panels (graphite or IR-black on thin metal panels). These can be driven with moderate power sources (solar?). Emissivity control, as mentioned, is trickier and specific materials should be investigated.

2.4.3 Proposal C: A thermal interferometer for Earth Observing

2.4.3.1 Rationale

The exploitation of the interferometric beam-combination to improve the angular resolution can take many forms. In this case, given the low sensitivity that a small and relatively cheap camera can offer, a thermal imaging camera could be pointed towards the ground (Earth) while receiving combined beams from two apertures.

2.4.3.2 Scope

Proof that this technique is viable in the thermal infrared could open the possibility (given sufficiently fast detectors) to design a future satellite of modest size but with extendable arms (and small dishes at the extremities) to provide high-spatial thermal resolution on the ground without having to resort to extremely large dishes.

2.4.3.3 Method

A 3U would be necessary for this concept: with two small collecting optics on each of the external units and the camera core in the center one. (see Figure 8). Simple scanning of the satellite pointed to the ground should provide sufficient information to allow collection of data with a synthesized beam with a factor of 10 greater than if the camera lens ~2cm were pointed at the ground.

2.4.3.4 Technology

Among the issues with this proposal is the need for a pressurized central part (for the camera and electronics), data rate transfer (most commercial cameras 120x160 or 240x320 have a 30Hz acquisition with an 8 bit dynamic range). The latter suggests a data rate short of 20Mb/s... so we could decide to reduce the portion of camera read to a small amount of pixels (20x20) for a 100kbit/s.
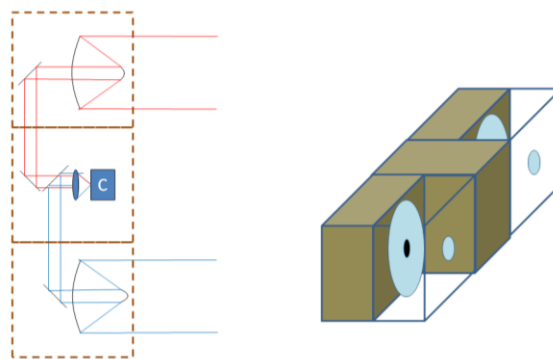

Figure 8 - Concept diagram of how a dual input synthetic interferometer 3-Unit cubesat would look like. The camera core and optics (C) could also be replaced by a single MIR or LWIR photodiode if the complexities of the design are excessive.

2.4.4 Proposal D: Hypertelescope

2.4.4.1 Scope

We propose to build an extremely simple nano-satellite demonstrator of what a multi-aperture imaging interferometer could achieve. Apart from one of the high-precision guiding probe on the Hubble Space telescope, it would, to the best of our knowledge, be the first ever space-borne interferometer.

2.4.4.2 Concept of multi-aperture interferometer

While a dual aperture (2A) system is at first glance less complex than a triple (3A) or more (nA) system, the requirement for full imaging capabilities sets much more stringent performance requirements, hence complexity and cost, to a 2A system. Indeed, while 2A systems require absolute measurement of pupil geometry to quarter-

wave accuracy (order of a micron for a 10μm system), in a 3A or more systems, which can deduce this absolute knowledge from the scientific measurements themselves thanks to the closure phase, requirements for absolute pupil geometry control is reduced to the order of Rλ where R is spectral resolving power and λ is wavelength. For R=1000 at λ=10μm, the pupil geometry controlled requirement is of the order of a cm, hence significantly reducing system complexity.

Multi-pupil interferometric recombination systems can become extremely complex, but this is not necessarily the case. The hyper telescope recombination scheme, following the original idea proposed by Labeyrie (A&A 1996), where all pupils are brought to interfere in a common focal plane creating a complex two-dimensional interference pattern, provides a simple and efficient recombination scheme without the use of beam splitters. Individual apertures, in the form of reflectors carried by free-flying or structurally interconnected spacecrafts located on a curved surface, can focalize light towards a common focus where the interference pattern is recorded using a bi-dimensional detector array. The focal plane spacecraft could potentially just contain a detector, but will in practice contain beam collection and exit-pupil arranging optics. The hyper telescope exit pupil does not need to reproduce its entrance pupil. In particular, the exit pupil could be densified, as in Labeyrie's original proposal (and in Michelson's famous experiment). In a scheme appropriate for a general imaging facility like FIRI, we believe the entrance pupil should be fully redundant, allowing for as many u-v points as possible to be collected in a single image. Making the pupil geometry evolve over time, the u-v plane for a given instrument pointing would be built up during the course of the observation.

2.4.4.3 Nanosat configuration

We propose to construct a nano-satellite version of a FISICA hypertelescope. To simplify, we would avoid free-flyers by selecting an object that can be observed with sufficiently small baselines to fit all in a small box: the Sun. Observed at 10μm, the sun is unresolved by millimetric apertures and resolved by a decametric aperture. The concept would consist of a 100mm-baseline hypertelescope composed of, seven 1mm diameter apertures feeding an infrared array detector. This would provide 21 baselines per image.

This system would fit into a 3U cube sat, with one unit for the telescope, one unit for the detector system (a Nano640E un-cooled array), and one unit for the satellite functions. A simpler option could consist of a visible webcam with a scaled-down aperture mask in front of it, essentially 0.1mm holes for a 10mm diameter telescope. This could possibly fit into a 1U cubesat.

The system would demonstrate fringe stability and capacity to record and combine baselines to reconstruct an image. A parallel camera could be implemented to record real images simultaneously (on the same detector) for reference. We could possibly also implement a second interferometer channel with only two apertures, allowing a comparison of the two interferometer concepts.

2.4.4.4 Basic interferometric considerations

We consider a 7-aperture system to observe the Sun from Earth orbit at 10μm. We choose aperture size (D) in order to not resolve the sun (full sun within the aperture main diffraction lobe FWHM). Hence, for λ/D = 0.5°, D = 1.14mm. We fix D=1mm.

The size of the nanosat fixes our baseline to B=100mm, allowing a final resolution element 100 times smaller. The total number of resolution elements on the sun surface is therefore (B/D)^2 π/4 = 7900.
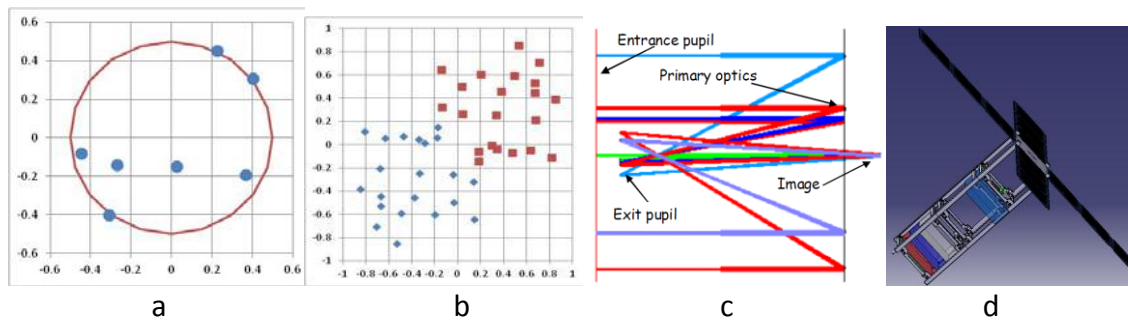

Figure 9 – a) Proposed aperture distribution. b): Instantaneous u-v plane coverage. c): First-cut ray-tracing of the HyperCube. d): First-cut mechanical design in a 3U CubeSat.

2.4.4.5 Entrance Pupil Arrangement

An n-aperture, non-redundant pupil provides N=n(n-1)/2 baselines. Our n=7 system therefore gives N=21 baselines in a snapshot. We can arrange the pupils in such a way as to make sure no two baselines are equal, and that they sample evenly the baselines from an inner minimum baseline b to the maximum baseline B. If we assume a polar orbit allowing pointing the sun during a complete orbit, stabilizing the satellite such that one of its sides always faces the earth then gives a rotation of the entrance pupil with respect to the sun of 360° in typically 1.5h, providing a full coverage of the u-v plane. For B=100mm and b=20mm, the N=21 baselines give a radial sampling of (B/b)/(N-1)=4mm. One possible aperture distribution is shown in Figure 9 (a).

2.4.4.6 Exit Pupil Arrangement

Several options can be taken for the exit pupil arrangement. The simplest option is to do nothing, in which case the longest baseline will produce 100 fringes across the unresolved solar image. If all the apertures are perfectly phased this arrangement may give some kind of image of the solar disk. In the absence of phasing, just making sure optical paths are coherenced, ie within the coherence length L=λ2/Δλ=Rλ, The image will be a collection of some 7900 speckles from which the u-v plane information (21 visibilities and phases) can be retrieved by Fourier analysis. Retrieving this information requires at least four detectors per speckle, ie an array of 200x200 detectors.

We can reduce the number of speckles, hence detectors, in the image by densifying the pupil: increasing the size of each individual pupil relative to their separation reduces the size of the unresolved image while maintaining the fringe spacing. The optimal amount of densification must be determined through end-to-end modelling which will be done in collaboration with UCL. The main parameter here is detector noise, see estimation below. We consider an exit pupil densified by a factor 5, reducing the number of detectors to 40x40 = 1600.

We can also rearrange the aperture pattern: as long as both entrance and exit pupils are redundant we can recover the on-sky u-v points after Fourier analysis of the recorded image. In our case, where we need 7 optical elements precisely positioned in the 20mm diameter exit pupil, we propose to place the apertures regularly spaced on

a circle, hence optimizing space while remaining non redundant. There is also a choice to be made between pupil-plane and image-plane recombination; to be further studied.

2.4.4.7 Detector and preliminary power budget

We propose to use the ULIS Nano640 un-cooled bolometric array with 640x480, 25µm pixels. This array, while never flown, is space qualified by CNES in preparation for missions such as Marco Polo-R. It provides a noise equivalent temperature difference at 300K of NETD<60mK, which corresponds to a noise equivalent power of some 20pW. For our 40x40-detector images, we therefore collect a total noise power of 0.8nW. Observing the sun from earth orbit at 10µm with a 10nm wide filter (R=1000) through 7 holes of 1mm diameter we collect a total of 30nW. As a first-order design this appears reasonable, but further analysis and optimization will be performed in the early design phase.

2.5   Critical analysis

Each proposal (A to D) described in Sections 2.4.1 to 2.4.4 have been rated using the following criteria:

- Interest for FISICA (weight 4): either directly applicable (e.g. interferometry techniques, formation flying, …) or strongly relevant (e.g. pointing stability, noise issues, …);
- Novelty (weight 3)
- Technological Readiness Level (TRL) gain (weight 3): this excludes the novelty but includes the potential industrial gain.
- Scientific interest (weight 2): by scientific here we refer mainly to astronomical or observational data prodcuts.
- Feasibility (weight 3)

Table 6 summarizes the evaluation of each proposal.

Table 6 – Proposals rating

	Weight	Proposal A: Accelerometer	Proposal B: Steering for thermal absorption/emission	Proposal C: Interferometer for Earth Observation	Proposal D: Hypertelescope
Interest for FISICA	4	2	2	2	2
Novelty	3	2	3	3	3
TLR gain	3	3	2	2	3
Scientific interest	2	1	1	2	3
Feasibility	3	1	2	1	2
TOTAL		28	31	30	38

Proposal A is interesting since it intends to validate a key technological brick (the high-precision accelerometer) involved in the formation flying control loop. However, our current knowledge on the operational conditions (orbits, stabilization, and thermal stability) is not sufficient to guaranty the complete validation of the accelerometer with the nanosat platform. Indeed, orbits and attitude that can be achieved will

generate both low and high frequencies disturbing the output of the accelerometer. Furthermore, the thermal environment will not be stabilized and the accelerometer will be affected by these temperature variations (then adding another noise). Therefore, a nanosatellite fully dedicated to the validation of the accelerometer seems too risky at this time.

Proposal B intends to demonstrate a promising method based on thermal emission for fine navigation while avoiding mechanical moving parts and combustion-based systems. The proposed payload is quite simple and could fit in 1U (even if the 3U configuration is preferred to enhance the torque effects).

Proposal C describes a thermal interferometer observing Earth. This payload is not complex except for 1) the optical path which has to be accurately maintained since the temperature will not be controlled in the nanosat; and 2) the camera which has to be pressurized.

Proposal D is the most interesting for both its capacity to provide a very first demonstration of space-based interferometric imaging; and its feasibility within the nanosatellite constraints. This payload is simple, mature and does not require stringent operational conditions.
It is worth noting that there would be sufficient volume, weight, and power allocations within a 3-unit cube-satellite to include the accelerometer (Proposal A) within the nanosatellite. This would also optimize the mission profile, since the current Proposal D would need very little observing time (essentially one orbit) while it would require a long lifetime for data transmission. The concept would therefore allow for long-term measurements of accelerometric data, and allow for the use of on-board navigation capacities already present on the platform in order to provide stability and controlled excitation movements of the satellite.

3   Conclusions and future steps

While the Proposal D was considered a strong case for a nanosatellite demonstration experiment, allowing for the first time demonstration of interferometric imaging in space, it was felt that its case in terms of technology readiness improvement was insufficient. The combination of the proposals D and A into a single, 3-unit cube satellite was found to provide an optimal mission concept.
This combined proposal will be the basis of the FISICA nanosatellite demonstrator study.